Modeling, Simulation, and Optimization of Hybrid Fe(II)/Fe(III) Redox Flow Fuel Cell System

Hossein Hojjati, Kalin Penev, Victor R. Pupkevich, and Dimitre G. Karamanev
Dept. of Chemical and Biochemical Engineering, University of Western Ontario, London, ON N6A 5B9, Canada

DOI 10.1002/aic.13988
Published online February 20, 2013 in Wiley Online Library (wileyonlinelibrary.com)

The kinetic parameters of ferrous iron oxidation, covering both lag and growth phases at low pH, were determined using a free suspended culture of the bacterium Leptospirillum ferriphilum. A mathematical model was developed to simulate the dynamics of a continuous bioreactor used for operation of a novel hybrid Fe(II)/Fe(III) redox flow fuel cell system. By changing the current load within a predefined range, three runs were performed to predict time-varying ferrous iron concentration, bacterial cell concentration, and pH as the major output variables of simulation program. The model was experimentally validated through three runs. It was found out that the key variable in dynamic analysis of the bioreactor was the current load applied. To optimize the bioreactor and the fuel cell conditions for a normal-steady-state operation, the optimal current profile for a transient phase was determined. A selected optimal policy was also implemented and validated during the mini-pilot-scale system experiments. © 2013 American Institute of Chemical Engineers *AIChE J*, 59: 1844–1854, 2013

Keywords: mathematical modeling, dynamic optimization, iron biooxidation, kinetic modeling, Leptospirillum ferriphilum, microbial fuel cells

Introduction

The past few decades have seen an ever growing interest in the development of novel energy technologies in two major directions: finding energy sources alternative to fossil fuels and increasing the efficiency of the energy conversion from the available primary energy sources. Fuel cells are a good example of the latter approach—the energy of the chemical reaction between a fuel (e.g., hydrogen) and an oxidant (typically oxygen or air) is directly transformed into electrical energy in an electrochemical device, similar to a battery. The fuel is continuously oxidized at an anode, releasing electrons that flowing through an external circuit to produce electricity and to reduce the oxidant at the cathode. Because there are no moving parts or intermediate stages in conversion of the chemical energy, the efficiency of a fuel cell can be much higher than that of heat engines, for example, microturbines. At the same time, the major disadvantage of fuel cells is the fact that the electrochemical reactions occurring therein require the presence of a catalyst or operation at elevated temperatures. In contrast, a redox flow cell is a device with a similar construction that uses a spontaneous electrochemical reaction between paired redox couples with a large redox potential difference, such as Fe^{2+}/Fe^{3+} and Ce^{2+}/Ce^{3+}. External energy can be used to regenerate the cathodic and anodic reagents; therefore, redox flow cells are typically used as energy storage devices. However, if a suitable fuel and/or oxidant are used for the regeneration purposes, the redox cell will work as an indirect fuel cell. The system, discussed here, is a hybrid between a fuel cell and a redox flow cell: hydrogen gas (H_2) is oxidized at the anodic side (Eq. 1), while ferric iron is reduced at the cathodic side (Eq. 2), which works as a redox flow half-cell based on the ferric-ferrous iron (Fe^{3+}/Fe^{2+}) redox couple. The cathodic and anodic compartments are separated by a polymer electrolyte membrane (PEM). The catholyte (iron sulfate solution in sulfuric acid, pH ~1.0) is regenerated in an external bioreactor using atmospheric oxygen with the help of iron oxidizing bacteria (Eq. 3).

$$\text{At the anode}: \quad 1/2H_{2(g)} \rightarrow H^+_{(aq)} + e^- \tag{1}$$

$$\text{At the cathode}: \quad Fe^{3+}_{(aq)} + e^- \rightarrow Fe^{2+}_{(aq)} \tag{2}$$

Catholyte regeneration

$$2Fe^{2+}_{(aq)} + 1/2O_{2(g)} + 2H^+_{(aq)} \xrightarrow{\text{(Iron oxidizing bacteria)}} 2Fe^{3+}_{(aq)} + H_2O_{(l)} \tag{3}$$

The thermodynamic characteristics of all reactions taking place in the hybrid fuel cell system are discussed in Supporting Information, Appendix A.

The iron oxidizing bacteria are autotrophic microorganisms that use atmospheric carbon dioxide as their sole carbon source and the ferrous iron oxidation (Eq. 3) for their energy supply. In the course of the oxidation process, the bacterial cells constantly divide and biomass is accumulated. The overall system—a hybrid between a fuel cell and a redox cell (redox fuel cell) with an integrated bioreactor—has been previously described by Karamanev et al.[1,2]

Additional Supporting Information may be found in the online version of this article.

Correspondence concerning this article should be addressed to D. G. Karamanev at dkaramanev@eng.uwo.ca.

In the last decade, a significant effort has been made on modeling and simulation of PEM fuel cells. Several one-dimensional (1-D), 2-D, or 3-D theoretical as well as semiempirical models have been developed to study the dynamic or steady-state characteristics of PEM fuel cells, applied mostly in automotive power systems or stationary power plants. These approaches have been recently reviewed.[3–5] Overall, the performance of PEM fuel cells is mainly limited due to overpotential losses and is evaluated by voltage-current density outcomes under different conditions (e.g., temperature, composition and flow rate of streams, pressure, cathode and anode porosities, catalysts, channel configuration, and humidity). To implement these developments within the described redox fuel cell, a working model of the cathodic redox half-cell needed to be developed, in which the rate of the ferric iron reduction (Eq. 2) is determined by the electrical current withdrawn from the system. It means that the limiting reaction can be considered the catholyte regeneration (Eq. 3), that is, the biological ferrous iron oxidation in the bioreactor.

The kinetics of the biological ferrous iron oxidation has been intensively studied for different species, modes of operations, and conditions of cultivation. At present, the most important iron oxidizing bacteria are considered to be *Acidithiobacillus* (*At*.) *ferrooxidans* and the species belonging to the genus *Leptospirillum* (e.g., *L. ferrooxidans*, *L. ferriphilum*).[6–8] The *Leptospirillum* species generally have slower growth rates, but tolerate lower pH and higher redox potential of the medium,[7] which makes them more appropriate for the purpose of the electrochemical system, described above.

Regarding the modeling of the biological ferrous iron oxidation, we used the electrochemical-enzymatic model.[9] This model is derived from first principles and it accounts for both the ferric and ferrous iron concentrations, but it does not cover other factors, such as the temperature and pH effects. In general, those effects are specific to the individual species or even strains of bacteria, and depend on the mode of operation: continuous or batch, with freely suspended or immobilized microorganisms. For example, the temperature effect on the cultivation of *L. ferriphilum* has been examined by several groups, and the optimal temperature for cultivation has been found to vary between 37 and 40°C.[10–12] The bacterial strain, used in our system, has already been kinetically examined under identical cultivation conditions by our group.[13] These findings were used in the overall modeling.

The difference between the rates of electrochemical ferric iron reduction and the biological regeneration (Eqs. 2 and 3) determines the ratio between the ferrous and ferric iron in the system, and hence the redox potential (E_h) of the solution (Eq. 4)

$$E_h = E' - \frac{RT}{nF} \ln \frac{[Fe^{2+}]}{[Fe^{3+}]} \tag{4}$$

where E' is the conditions-dependent formal redox potential, R is the universal gas constant, T is the absolute temperature, n is the number of electrons exchanged in the reaction, and F is the Faraday constant; $[Fe^{2+}]$ and $[Fe^{3+}]$ denote the ferrous and ferric ion concentrations, respectively.

The formal potential for the ferrous/ferric system at pH ~1.0 (in sulfuric acid) remains nearly constant, around 0.67 V vs. standard hydrogen electrode (SHE).[13] However, the redox potential of the catholyte can be much higher, approaching 1.00 V vs. SHE.[7] This value is slightly lower than, but comparable to the standard redox potential of the oxygen reduction reaction (Eq. 5), which is 1.23 V. The difference accounts for the energetic needs of the bacterium and thermodynamic losses.

$$O_{2(g)} + 4H^+_{(aq)} + 4e^- \rightarrow 2H_2O_{(l)} \quad E^0 = 1.23 \text{ V vs. SHE} \tag{5}$$

The redox potential of the catholyte determines directly the voltage of the electrochemical cell and, ultimately, its efficiency and power output. Therefore, optimal operation of the redox flow fuel cell will require a high and constant redox potential, that is, low and constant ferrous iron concentration. The maximum potential, as aforementioned, is limited by the energetic requirements of the bacterial cells. A second limitation from the biological system comes in the need of maintaining the pH within a narrow range. Very low pH can inhibit or completely deactivate the iron-oxidizing bacteria, whereas high pH promotes formation of biogenic ferric precipitates, such as jarosite, $(K, NH_4, H_3O)Fe_3(SO_4)_2(OH)_6$. In addition, increased pH decreases the diffusivity of the ferric iron and hinders the cathodic process likely due to formation of polyatomic complexes.[14] The latter restriction is particularly important for operation under transient conditions: as seen from reactions (2) and (3), protons are involved in the processes, so the pH decreases when the ratio between ferrous and ferric iron increases and vice versa. For this reason, thermodynamic prediction of the pH of the solution during transient operation will also be included in the final model of the system.

Considering the aforementioned, the current work was aimed at the development of a mathematical model capable of predicting the effects of a current drawn from a fuel cell on dynamics of the bioreactor and catholyte composition, and, finally, evaluation of the model by performing simulations and using real data.

Model Development

Ionic speciation and pH of the catholyte

Thermodynamic modeling of the ionic speciation of the catholyte solution was used to predict the changes in pH during the operation of the system. The model details can be found in Supporting Information (Appendix B: pH Modeling).

Kinetic model for the ferrous iron oxidation

For microbial processes, the exponential growth phase of batch cultivation can typically be modeled using the Monod equation. However, the biological iron oxidation involves an electrochemical equilibrium at the surface of the microbial cell membrane and, therefore, the applicability of the Monod model is not straightforward. A few models have been developed for such an oxidation reaction and reviewed by Ojumu et al.[15] In our view, electrochemical-enzymatic model[9] developed for *A. ferrooxidans* is the most complex and complete model; it is based on the enzymatic and electrochemical equilibria at the surface of the cell membranes of the iron-oxidizing microorganisms. The model gives the following relationship for the specific ferrous-iron oxidation rate

$$q_s = -\frac{1}{X}\frac{d[Fe^{2+}]}{dt} = \frac{q_{max} - K_2 \frac{[Fe^{3+}]}{[Fe^{2+}]}}{1 + K_S \frac{1}{[Fe^{2+}]} + K_1 \frac{[Fe^{3+}]}{[Fe^{2+}]}} \tag{6}$$

where q_s and q_{max} are the specific and the maximum specific ferrous iron oxidation rates, respectively; X is the bacterial

cells concentration; and K_1, K_2, and K_S are the kinetic constants of the model that have to be determined using experimental data. Assuming a constant biomass yield coefficient, Y, the specific growth rate, μ is given as

$$\mu = \frac{1}{X}\frac{dX}{dt} = q_s \cdot \ Y \tag{7}$$

Using a previous kinetic study of the same species of *L. ferriphilum*,[13] the mean oxidation rate was determined to change linearly with pH within the range of 0.7–1.1. The linear variation can be related to a change of the maximum specific oxidation rate

$$q_{\max} = \alpha(\mathrm{pH}) + \beta \tag{8}$$

where α and β are the constants that have to be estimated from the experimental data obtained in that study. Further, it was shown that during batch cultivation, various lag times were observed within a predefined range of pH and total iron concentration. During the lag phases, ferrous iron biooxidation did occur and it proceeded with an almost constant rate showing very low cell division rate. In contrast, during the exponential growth phase, strictly growth associated ferrous iron biooxidation was seen and the yield coefficients for each run were mainly constant.[13] Such variations should be included in kinetic study to analyze the process under the unsteady-state conditions.

In a batch operation mode, the conservation equations for bacterial cells and the ferrous iron concentrations can be written as

$$\frac{dX}{dt} = (1-e^{-kt})\mu X \tag{9}$$

$$\frac{d[\mathrm{Fe}^{2+}]}{dt} = -\frac{1}{Y}\mu X \tag{10}$$

The right-hand side of the bacterial cells concentration balance is multiplied by $(1-e^{kt})$ term, representing the contribution of the lag phase in the cell growth rate. In this term, t is the time and k represents reciprocal of a time constant (τ) for the lag phase, which describes how fast the lag phase moves toward the cell growth phase. At early stages of operation, the term is close to zero resulting in a very low cell division rate; whereas, for $t \succ 3\tau$, the term approaches unity, representing the exponential growth phase of cell growth. The results from the previous study can be interpreted to show that the value of k was a function of initial pH ($\mathrm{pH_o}$) and initial ferrous iron concentration ($[\mathrm{Fe}^{2+}]_o$). The following empirical equation relating the above parameters provided the best fit to our experimental results

$$k = c(\mathrm{pH_o})^d([\mathrm{Fe}^{2+}]_o)^f \tag{11}$$

where c, d, and f are the constants that should be estimated.

Dynamic model development of the integrated bioreactor-redox flow cell system

The major equations, describing continuous bioreaction dynamics, include the bacterial cells and ferrous iron balances. Assuming a well-mixed system (the output concentration and the concentration within the system are equal), constant volume, and constant temperature, the following equations can be written

$$\frac{dX}{dt} = (1-e^{-kt})\mu X \tag{12}$$

$$\frac{d[\mathrm{Fe}^{2+}]}{dt} = \frac{v}{V}([\mathrm{Fe}^{2+}]_{in} - [\mathrm{Fe}^{2+}]) - \frac{1}{Y}\mu X \tag{13}$$

where V and v are the volume of the bioreactor and the recirculation rate of the solution through the fuel cell, respectively. The input and output terms of the bacterial cells balance equation are assumed to be equal (no growth in circulation lines and the fuel cell); whereas, the difference between the input and the output terms of ferrous iron concentrations can be related to the electric current, I, generated by the fuel cell

$$v([\mathrm{Fe}^{2+}]_{in} - [\mathrm{Fe}^{2+}]) = 3600\frac{IM_{\mathrm{Fe}}}{nF} \tag{14}$$

where n, F, and M_{Fe} are the number of electrons participating in the electrochemical reaction ($n = 1$ in our case), the Faraday constant, and the molar mass of iron, respectively; 3600 is the conversion factor for the time unit. Substituting Eq. 14 in Eq. 13 results in an equation in which ferrous iron concentration changes within the bioreactor are independent of the recirculation rate and is a function of an applied current load. In fact, at constant current, an increase in the recirculation rate decreases the fuel cell outlet ferrous iron concentration, but the molar rate of ferrous iron addition into the reactor remains constant.

Because the total iron concentration, $[\mathrm{Fe}]_t$, and the volume are constant, the ferric iron concentration can be calculated as follows

$$[\mathrm{Fe}^{3+}] = [\mathrm{Fe}]_t - [\mathrm{Fe}^{2+}] \tag{15}$$

Limitations of the model

According to Penev and Karamanev,[13] the optimal biooxidation and cell growth rates can be achieved within the pH and temperature ranges of 1.05–1.80 and 38–42°C, respectively. Our experience, however, shows that working at such pH conditions leads to precipitation of ferric iron complexes in the bioreactor, causing problems such as scaling and clogging. Although, as expected, both rates decreased linearly, no solid particles formation was observed at varying pH within 0.70–1.05 range, which was chosen for the experiments described here.

Carbon dioxide and oxygen availability in the bioreactor solution are other limitations, which may need to be considered in the modeling approach. Recently, it has been shown that for *L. ferriphilum* cultivated under similar conditions: freely suspended in a well-mixed reactor, the CO_2 supply with atmospheric air is sufficient.[16] The dissolved oxygen concentration depends on the solution composition, temperature, aeration method (distributor type), and the air flow rate. Even under optimal bioreactor conditions, the oxygen mass transfer could limit the maximum current obtainable from the hybrid electrochemical cell. The limitations were investigated in a series of experiments performed in our mini-pilot-scale system. The results showed that the bioreactor could handle a maximum of 1.0 A current load per 1.75 L of bioreactor volume. For the loads higher than the maximum value, the oxygen mass transfer becomes the limiting process of the system, which results in a decrease in biooxidation rate, an increase in ferrous iron concentration, and a decrease in pH of the catholyte. In turn, these changes further inhibit the biological iron oxidation reaction and, ultimately, make operation of the system unstable with a positive feedback

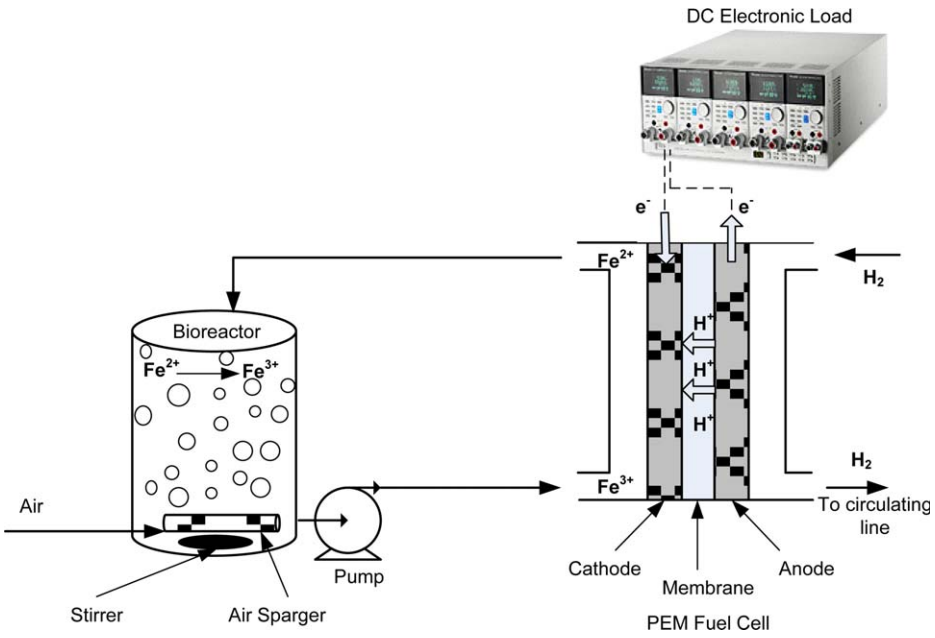

Figure 1. Experimental setup of bio-fuel cell system.

[Color figure can be viewed in the online issue, which is available at wileyonlinelibrary.com.]

mechanism in action. Therefore, for the purpose of this study, the pH range and the maximum current drawn were necessarily limited to the values declared above. The solution temperature was kept within the range of 39–40°C.

Since the recirculation rate of the catholyte through the redox flow fuel cell may affect its performance by causing concentration polarization that was maintained (for all the fuel cell types used) at such a level to provide a catholyte residence time in the electrochemical cell ~1.75 s.

Materials and Methods

Bacterial culture and growth media

The main source of the microbial culture, *L. ferriphilum*, was provided from acid mine drainage of Iron Mountain Mine (Redding, CA), and has been cultured in our laboratory since 2005. Solutions with required total iron concentration were prepared by dissolving an appropriate mass of analytical-grade $FeSO_4.7H_2O$ in deionized water, and then pH was adjusted with concentrated H_2SO_4. A solution containing $(NH_4)_2SO_4$, K_2HPO_4, $MgSO_4{\cdot}7H_2O$, and KCl was added to the system to get a final concentration of 0.40, 0.05, 0.10, and 0.01 g/L in the bioreactor liquid for each salt, respectively.

Analytical methods

A transmitted light optical microscope Axioskop 40 (Carl Zeiss, Germany) with 1000× magnification equipped with a camera and image acquisition software was used to determine the cell concentration through direct manual counting. For the cell concentrations less than 2×10^{10} cell/L, cell numbers were counted directly in a sample taken from the bioreactor. Otherwise, the sample was diluted 2–6 times and then cells were counted. An average of 10 counts from pictures taken in different spots on a microscope slide was considered to be an average microbial cells concentration in the bioreactor liquid. The absolute error of a counting method was expected to be 4×10^9 cell/L in the range used in this study.

Following the same procedure described by Penev and Karamanev,[13] UV-vis spectrophotometery (Cary 50, Varian) was used for the determination of total iron and ferric iron concentrations of less than 0.15 g/L. Otherwise, the ferrous iron concentration was determined by titration with 0.1 N $K_2Cr_2O_7$ (VWR International, Canada) in ~10% sulfuric acid and using *N*-phenylanthranilic acid (Sigma Aldrich, USA) as a potentiometric indicator. The ferric iron, on the other hand, was titrated with EDTA (Sigma Aldrich) in an acetic acid-sodium acetate buffer (pH ~4) in the presence of 5-sulphosalicylic acid (Caledon Labs, Canada) as a complexometric indicator. The difference between total and ferric iron concentrations presented the ferrous iron concentration.

Orion Benchtop meter (Thermo Scientific) equipped with an Orion Ross® combination pH electrode with built-in temperature sensor was used to measure pH of the solution with the accuracy of 0.01. The dissolved oxygen concentration was occasionally measured with an Orion dissolved oxygen probe (Thermo Scientific).

Experiments

The data from the kinetic study on the ferrous iron biological oxidation carried out in a circulating bed bioreactor[13] were used for finding the parameters of the kinetic model described in the previous section. All other experiments regarding simulation and optimization sections of this work were carried out in a setup, schematically shown in Figure 1. An acid-resistant vessel was used as the bioreactor. Aeration and gentle mixing were achieved by sparging pressurized air through the bioreactor liquid. Throughout the experiment, the dissolved oxygen concentration ranged between 50 and 30% saturation (~3–2 mg/L). The solution temperature was maintained at 40 ± 0.5°C by circulating the heated water through an acid resistant coil immersed in the solution (not shown in the figure for simplicity).

Besides being mechanically robust and resistant to strongly oxidizing solutions containing ferric iron used at the catholyte, the membrane, as a core component of the hybrid fuel cell, must possess high proton conductivity. The effect of such solution on the proton conductivity of some proton exchange membranes was previously investigated by our group.[17] The contamination of proton exchange membranes such as Nafion (DuPont, USA) in the presence of iron ions was reported. However, a bipolar proton exchange membrane Selemion HSF (Asahi Glass Company, Japan) had the highest proton conductivity as well as showed the lowest sensitivity to contamination by iron ions in the acidic media. There was also no membrane fouling observed thanks to the design of the electrochemical cell and specifics of attachment of acidophilic bacteria to surfaces.[18] Thus, the Selemion HSF was used to separate the anodic and cathodic half-cells. Three different configurations provided with 16, 100, and 400 cm^2 effective electrodes working area for the hybrid cell. A variable flow rate pump was used to circulate the bioreactor solution through the cathode compartment. The hydrogen pressure in the anodic compartment was kept constant at 35 kPa (gauge) through a controlled supply of ultrapure hydrogen (grade 5.0) and recirculated through a condenser at flow rate of 15 L/min to remove any water that would pass through the membrane. The current, drawn from the redox flow fuel cell, was adjusted and controlled using DC electronic load (Chroma 6314, USA) through an open-loop control strategy. The voltage corresponding to the drawn current was also monitored.

To test and fine-tune the newly developed model, a series of experiments were performed in the operational hybrid redox flow fuel cell system, using reactors of different sizes (22 and 55 L). The bioreactors were started in a batch mode, using 40 g/L total iron concentration at pH from 0.7 to 1.0. Once all the ferrous iron got converted into ferric iron, the bioreactor solution started to be circulated through the fuel cell. Altering the fuel cell current load allowed to adjust the incoming concentration of ferrous iron into the bioreactor. At the onset of each run, the following initial parameters were measured: total and ferrous iron concentrations, bacterial cells concentration, pH, as well as the corresponding open and short circuit voltages, and the short circuit current of the fuel cell. At a start-up of the system, the DC electronic load was set at an open circuit mode and the catholyte was started to be circulated through the cell. Once the fuel cell voltage had stabilized, the selected current load, at $t = 0$, was implemented using the constant current mode of the electronic load. For $t > 0$ in different time intervals, samples of the liquid were taken from the bioreactor and the variables required for the further analysis were measured. During the operation of the hybrid cell, water losses were observed due to evaporation from the bioreactor and passage of water through the cell membrane. For this reason, an appropriate amount of deionized water, if necessary, was added to the bioreactor to compensate for those losses. In all cases, no iron was detected in water that had penetrated through the membrane.

Mathematical solver package

All technical computing was performed in MATLAB® environment. Required MALTAB codes were written to solve the described modeling equations in all stages. The set of linear and nonlinear equations were solved by using the *fsolve* command (Gauss–Newton algorithms with line-search method), whereas the *ode45* command (explicit Runge–Kutta) was applied to solve the set of ordinary differential equations. Optimization of all constrained nonlinear multivariable functions was done using the *fmincon* command (iterative method using a sequential programming to solve a quadratic programming subproblem and estimating Hessian at each iteration).

Results and Discussion

Kinetic parameter estimation

The equations describing the batch bioreactor dynamics are Eqs. 6-15. Their simultaneous solution gives the microbial cells and ferrous iron concentrations for both the lag and exponential growth phases. Through an optimization method and a simulation program, the predicted data corresponding to experimental data can then be applied to estimate the unknown coefficients of K_1, K_2, K_S, Y, α, β, c, d, and f. The error ($e_{i,j}$) between the jth value of ith measured variable ($y_{i,j}$) and its corresponding simulated value ($\tilde{y}_{i,j}$) is defined as

$$e_{i,j} = y_{i,j} - \tilde{y}_{i,j} \tag{16}$$

An objective function for the optimization method can be defined in such a way to minimize the sum of the square errors (model residuals). An important issue in formulation of the objective function is the scaling of the variables. Particularly, the measurement errors in the cell counting are much higher than those associated with the ferrous iron concentration determination. In general, the optimization on its own cannot recognize the order of magnitude, dimensions, accuracy of a value measured, and importance of each variable; hence, an objective function without proper scaling or weight factors may results in excessive sensitivity toward one variable (e.g., cell concentration) while ignoring other variables (e.g., ferrous iron concentration). Thus, the weighted least-squares method was used to overcome such problems. In this study, the weight factors were first scaled to bring the measurements of errors for both variables to the same order of magnitudes and then determined on a relative scale due to measurement precisions of cell counting and ferrous iron concentration described in pervious sections.

$$\min_{\theta} \Phi(\theta) = \sum_{i=1}^{N_m} \sum_{j=1}^{Ni} \omega_{i,j} e_{i,j}^2(\theta)$$

subjected to

$$\text{Eqs. 9–18}$$
$$\theta^L \le \theta \le \theta^U$$

where N_m is the number of variables and N_i is the number of measurements of each variable; θ and $\omega_{i,j}$ denote the parameter vector and nonnegative weight factor, respectively. In the optimization program, the latter was chosen small for variables measured on a large scale or measured with lower precision (e.g., cell counting). Otherwise, it was chosen large. Two variables—ferrous iron and bacterial cells concentrations—were included in the objective function. The modeling objective was to find a set of kinetic parameters that minimizes the square of errors between the measured and simulated values for the ferrous iron and the bacterial cells concentrations, subject to constrains imposed by the model equations and known boundaries (θ^L and θ^U) of the parameters for better and faster convergence.

Table 1. Estimated Parameter Values

Parameter	This Study	Penev and Karamanev (2010)
K^1	0.0206	0.0209
K^2	0.0000	Assumed to be zero
K_S ($g_{Fe^{2+}}/L$)	0.0150	0.0067
q_{max} [$g_{Fe^{2+}}/(cells \cdot h)$]		11.1×10^{-12}
α	22.0×10^{-12}	(average value)
β	-11.2×10^{-12}	
Y ($cells/g_{Fe^{2+}}$)	6.13×10^9	6.97×10^9
k (1/h)		–
c	0.0235	
d	0.6977	
f	6.9334	

For the estimation of the kinetic parameters, we used four of the five data sets from our previous kinetic study of the microbial ferrous iron biooxidation.[13] The last data set was applied to validate the developed model. The obtained estimates are presented in Table 1 and compared with the parameters determined by the previous study. The most interesting result of the simulation is the K_2 value. It is estimated to be zero, a value that was postulated in our previous work.[13] Also, the predicted coefficients for k (Eq. 11) show that the initial pH has greater influence on the lag phase than the initial ferric iron concentration.

The measured and simulated ferrous iron and bacterial cells concentrations are presented in Figure 2. For all data sets, the experimental and simulated ferrous iron concentrations are in a very good agreement for both lag and growth phases. However, small discrepancies are observed in the case of bacterial cells concentrations, which can likely be related to the corresponding weight factors applied for the less reliable experimental data, associated with cell counting. The ferrous iron and bacterial cells concentrations for the fifth data set was used to validate the model (see Figure S1 from Supporting Information, Appendix C). A reasonable agreement between the experimental and simulated values is observed for both phases as well.

Assuming zero value for the K_2 parameter as well as an average value for q_{max} (with no pH dependency), Penev and Karamanev[13] used a different approach to estimate the kinetic parameters only for the exponential growth phase; the lag phase was estimated by a linear function separately. For a comparison, their estimates are presented in Table 1. The observed differences in K_S, q_{max}, and Y parameters may be due to the different approach, taken in that work.

In general, the good agreement between the simulated and experimental data indicates that the model is well-defined.

Simulation

Model Solution. Once the coefficients of the kinetic model (Eqs. 6–8) as well as the k equation (Eq. 11) for the lag phase were well-defined, the pH modeling (see Supporting Information, Appendix B) and Eqs. 6–15 were applied to simulate the dynamics of a continuous bioreactor for any current loads within a studied range. Before the simulation runs were executed, the microbial cells, ferrous iron, and total iron concentrations as well as pH of the solution were measured. The sulfate concentration, $[SO_4^{2-}]$, was unknown, but it could be calculated using the measured initial conditions and the total charge balance equation (Eq. S10 from Supporting Information, Appendix B: pH Modeling).

Finding the sulfate concentration required solving a combination of linear and nonlinear algebraic equations (Eqs. S1–S12 from Supporting Information, Appendix B: pH Modeling) simultaneously in an iterative procedure. The procedure was repeated until the difference between two consecutive iterations for the summation became less than 1×10^{-4} $mole/kg_{water}$. Then, the calculated sulfate ions concentration and the summation of concentrations were saved for further calculations.

For $t > 0$ and constant electrical current loads, the explicit Runge–Kutta method was applied to solve Eqs. 12–14 and to predict the bacterial cells, ferrous iron concentrations, and pHs at any step size within the time interval $[t_0, t_f]$. First, the pH value, at a particular step size, was estimated by solving the combination of linear and nonlinear algebraic equations (Eqs. S1–S12 from Supporting Information, Appendix B: pH Modeling) simultaneously. Then, the estimated specific growth rate was used to determine the bacterial cells and ferrous iron concentrations for the next step size.

Simulation Results. Three simulation programs, S1–S3, were used at different initial conditions to show the effect of current variations on the dynamic behavior of the system (Table 2). The upper value of a current range was limited to either short circuit current (I_{sc}) measured at the onset of each experiment or maximum achievable current (I_{max}) accounted for by oxygen mass-transfer limitations.

For the first simulation, S1, the variations of ferrous iron concentration, cell concentration, and pH at different fuel cell current loads are sketched in Figure 3. The initial pH was selected to be close to its optimal value, corresponding to a relatively short lag time, and the cell concentration was fairly low (Table 2). The simulation shows that at current

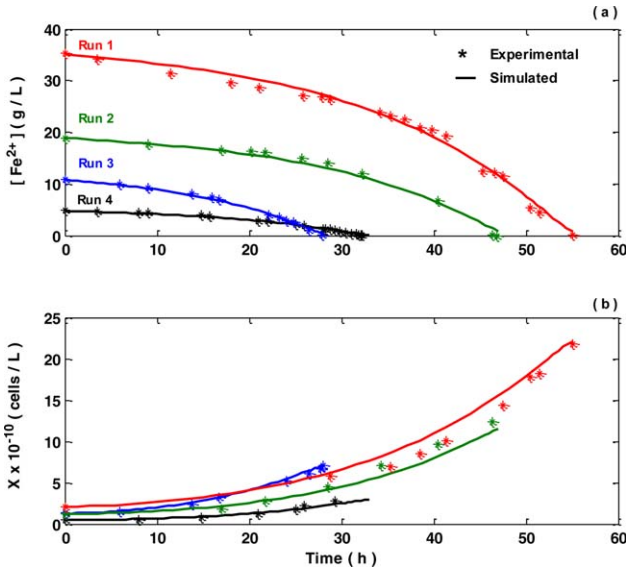

Figure 2. Comparison of experimental and modeling results for kinetic parameter estimation: (a) total ferrous iron concentration; (b) cell concentration.

[Color figure can be viewed in the online issue, which is available at wileyonlinelibrary.com.]

Run 1: $[Fe]_{t,o}$ = 38.2 g/L; pH_o = 0.89.

Run 2: $[Fe]_{t,o}$ = 20.8 g/L; pH_o = 0.95.

Run 3: $[Fe]_{t,o}$ = 10.8 g/L; pH_o = 1.08.

Run 4: $[Fe]_{t,o}$ = 5.3 g/L; pH_o = 1.08.

Table 2. Fuel Cell Dimensions and Initial Conditions Used for the Simulation and Optimal Current Profile Programs

	Initial Conditions			
	Simulations			
Variables	S1	S2	S3	Optimal Current Profile
V (L)	21.5	21.5	22.0	55.0
[Fe] (g/L)	44.0	43.5	40.4	45.5
[Fe^{2+}] (g/L)	0.00	0.00	0.10	0.14
X (cells/L)	4.8×10^{10}	10.6×10^{10}	14.2×10^{10}	20.2×10^{10}
pH	0.94	0.99	0.77	0.89
T (°C)	39–40	39–40	39–40	39–40
Fuel cell dimensions (cm × cm)				
Compartments	5.0×5.0	5.0×5.0	12.0×12.0	24.0×24.0
Electrodes	4.5×4.5	4.5×4.5	11.0×11.0	22.0×22.0
Effective surface area	4.0×4.0	4.0×4.0	10.0×10.0	20.0×20.0
I_{sc} (A)	8.1	8.1	14.5	35.4
I_{max} (A)	11.5	11.5	12.0	30.5
I (A)	1.0–4.5	2.0–5.0	5–11	–
I_s (A)	4.0	3.0	10.0	–

loads less than 3 A, the ferrous iron concentration would increase sharply, reach a peak value, and then gradually decrease showing a reasonable balance between the generation of ferrous iron in the fuel cell and its consumption by microorganisms. The ferrous iron concentration spike would be quite low, which would allow keeping the pH close to its initial value for a higher ferrous iron biooxidation rate. The cell growth kinetics would pass through a reasonably short lag phase before continuing in exponential growth. These conditions would lead to a smooth operation (steady state) in which an equal number of protons would be released from hydrogen oxidation (Eq. 1) and consumed by the bacteria (Eq. 3) resulting in a constant value for the average pH of the catholyte. The excessive biomass/microorganisms would be also harvested from the bioreactor by a process such as continuous centrifugation.

An increase in the fuel cell current load to more than 4 A, however, would result in a larger ferrous iron concentration spike at which the pH of the solution would drop significantly, leading to lower biooxidation and cell growth rates, and, ultimately, to unstable behavior of the system. In fact, either during start-up operation or high fuel cell current load condition, protons would generate faster from hydrogen oxidation (Eq. 1) than they would be consumed by the ferrous iron biooxidation reaction (Eq. 3) resulting in pH drop.

The second simulation, S2, was performed with improved initial conditions for the bioreactor. The cell concentration was relatively high, and the pH was even closer to its optimal value (Table 2). Figure S2 (see Supporting Information, Appendix C) displays the corresponding evolutions of ferrous iron concentration, bacterial cells concentration, and pH at applied current load ranging from 2.0 to 5.0 A. The simulation results show that the generation and consumption terms of Eq. 13 are well-balanced to minimize the deviation of pH from its initial value even for the highest current load applied, 5 A (the maximum deviation of pH was calculated to be 0.01). The ferrous iron concentration peak would be relatively low and it would appear at the early stages of operation due to the relatively short lag-phase time. As the bacterial growth phase would start considerably earlier, the microorganism concentration would reach a significantly higher level in shorter times as well. As a result, the generation rate of ferrous iron in the fuel cell would be just slightly higher than the rate of its oxidation by microorganisms. In comparison with simulation S1, a smooth operation of the fuel cell would be expected under the improved initial conditions even if the current load value was higher than 4 A.

For the third simulation, S3, a 22-L bioreactor containing the growth medium with moderately high bacterial cells concentration (Table 2) and the fuel cell with 100 cm^2 electrodes working area capable of producing 14.5 A at short circuit, I_{sc}, was used instead of 16 cm^2, as in two previous runs. The upgraded fuel cell allowed for increasing the applied operation current range to 5–11 A. The pH of the solution, however, was adjusted to 0.77 to investigate the process responses at low pH as well as ability of the model to predict ferric and ferrous iron concentration at pH below the lower limit of 0.7, selected for this study. The evolutions of the same variables for simulation S3 are presented in Figure S3 (see Supporting Information, Appendix C). Because of the low initial pH, the microorganisms would show a longer lag-phase time (no major growth would be observed within first 50 h). At the same time, working at low pH would lead to a decrease in the biooxidation rate of ferrous ions, that is, slower generation of ferric iron. For applied current loads less than 6 A, in spite of very low biooxidation and microorganisms growth rates, the initial cells concentration would be high enough to handle amounts of the ferrous iron generated in the fuel cell and, consequently, to keep the pH fairly close to its initial value. However, for current loads higher than 6 A, the amount of generated ferrous iron would hike rapidly, which would result in an increased ferrous iron concentration and, ultimately, in a drop of pH below 0.7, leading to a very poor overall performance of the system.

The validity of the model within predefined ranges can be assured if the simulated program outcomes are comparable with corresponding variables measured during experimental runs, in which a selected constant current, I_s, from the applied current load range was implemented. Three runs, R1–R3, for the current load values 4, 3, and 10 A were selected to be implemented at the onset of experiments in which the initial conditions were the same (Table 2) as those applied in simulations S1, S2, and S3, respectively. At all stages of each run, the circulation rate, the withdrawn current, and the inlet and outlet ferrous iron concentrations were measured, and the change of the ferrous iron concentration was predicted using Eq.14. A very good agreement between the predicted and measured values was observed

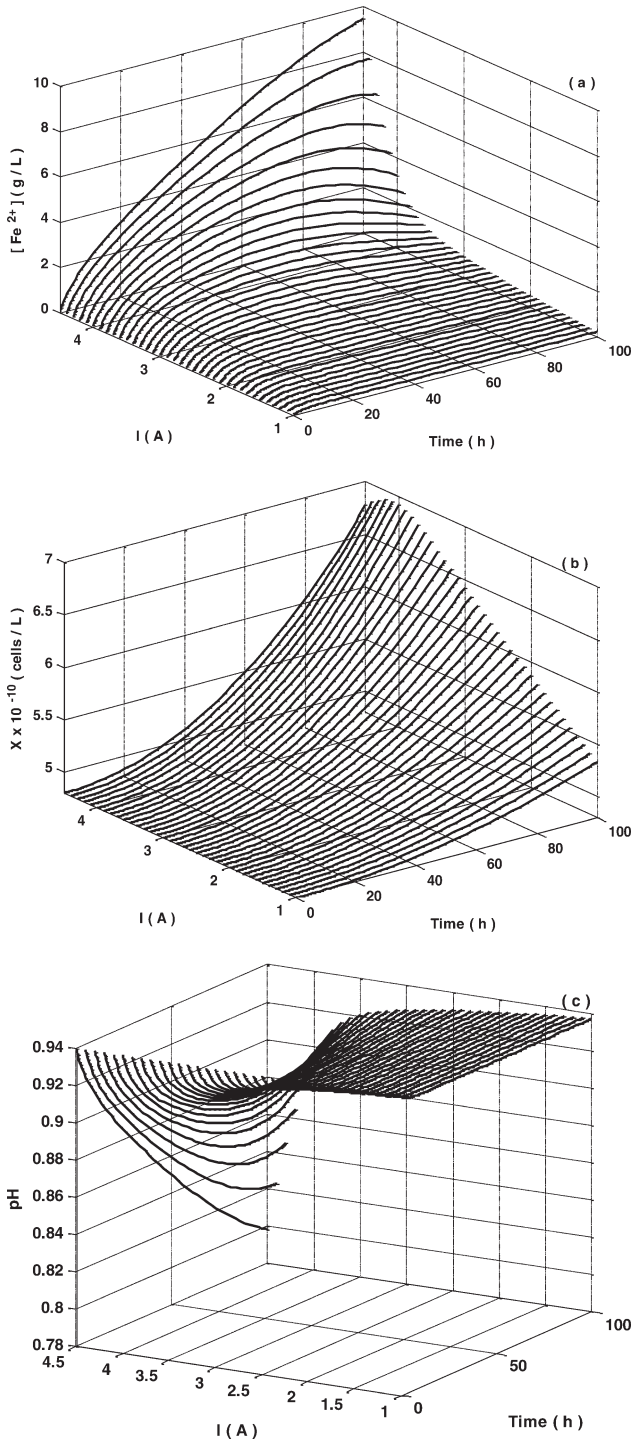

Figure 3. Results of simulation S1: (a) total ferrous iron concentration; (b) cell concentration; (c) pH.

(see Supporting Information, Appendix D) to validate 100% cathodic current efficiency assumption behind the model.

Figure 4 depicts the experimental and predicted results at the aforementioned applied current loads. It can be seen that all simulated ferrous iron concentrations, bacterial cells concentrations, and pHs are in a reasonable agreement with experimental data. Although the pH values are slightly overestimated for all runs, those are still within the range specified for accuracy of the pH measurement. The apparent overestimation of pH may be caused by some of the simplifications taken in the activity coefficients model (see Supporting Information, pH Modeling).

For the first run, R1, the ferrous iron concentration was slowly increasing at the beginning of the experiment and reached its maximum of ~4 g/L after 60-h operation, then gradually decreasing until the experiment ended. The fuel cell still was able to operate at constant current of 4 A during the concentration peak, though a considerable drop in the voltage due to an increase in ferrous ions concentration was observed. The fuel cell performance, however, was improving when the ferrous iron concentration started decreasing after 60 h of operation. The small drop in pH did not significantly affect the ferrous iron biooxidation rate resulting in a reasonable bacterial cells growth rate after a comparatively short lag time. For the second run, R2, no major variations of the ferrous iron concentration and pH were noticed, therefore, a smooth operation for both the fuel cell and bioreactor was observed. After passing a lag phase that was shorter than the corresponding lag time in run R1, the cell growth rate was reasonably augmented and improved the regeneration of ferrous iron. The experimental results for the run R3, however, showed a worse scenario in operation for both the bioreactor and fuel cell. The low initial pH provided a long lag phase during which no major increase in a bacterial cells concentration was observed. Although the initial cell concentration for this run was the highest among the experimental runs (Table 2), the ferrous iron concentration sharply increased and caused the pH to drop below 0.7 resulting in a relatively low ferrous iron biooxidation rate. In turn, the high ferrous iron concentration resulted in a voltage decline to a level at which the redox potential of the solution was not high enough to keep the current constant at 10.0 A and, which consequently, led to unstable operation and shut down of the system. It can also be seen that the experimental results do not agree well with simulated outputs for pH less than 0.6. The deviation can be accounted for by the nonlinear dependence between the ferrous iron biooxidation rate and pH at that pH value, as shown by Penev and

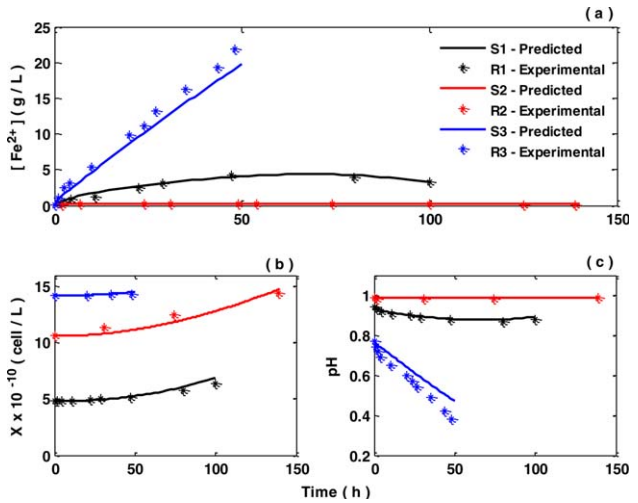

Figure 4. Comparison of experimental and simulation results for currents (I_s) selected within the applied current ranges of simulations S1, S2, and S3: (a) total ferrous iron concentration; (b) cell concentration; (c) pH.

[Color figure can be viewed in the online issue, which is available at wileyonlinelibrary.com.]

Karamanev[13]; in contrast to the linear dependence (Eq. 8) used in this study.

Overall, a good agreement between the predicted and measured variables indicates that the model was well-identified within the predefined ranges of variables. All the results, simulated and experimental, indicate that the implemented current loads should be selected with great care in order not to imbalance the system, that is, the ferrous iron concentration should be kept at a minimum possible level for a better fuel cell performance, but still high enough (higher ferrous iron concentration creates favorable conditions for microorganisms, provided that the pH is kept within an optimal range for their growth) to provide efficient bioreactor operation. The initial pH and initial microbial cells concentration have to be considered as factors influencing a choice of implemented current load, because they have a significant effect on the length of a lag phase. Therefore, an optimal current profile for a transient phase of operation is required to achieve a smooth steady-state operation at which an even balance between generation and consumption of ferrous ions and no significant pH changes are observed, while the maximum attainable current is being drawn from the system.

Optimal current profile

The goal of the optimization is to achieve the maximum attainable current as fast as possible without creating an unstable condition for either the bioreactor or the fuel cell. Applying the maximum current load at the onset of operation would result in a sharp increase in a ferrous iron concentration on early stages of operation, which would lead to a significant pH drop. Although the high ferrous iron concentration is favorable for the microorganisms, lowering a pH decreases the rate of biooxidation, which may cause an unstable condition. In addition, a high ferrous iron concentration reduces the redox potential of the catholyte (based on Eq. 4) and increases the concentration polarization within the fuel cell. So, a high ferrous iron concentration results in two negative effects that lower performance of the fuel cell (e.g., decrease the maximum attainable current). Determination of a maximum ferrous iron concentration for the fuel cell as a limit for optimization program is out of the scope of this study and we assume that the value has been given.

The general statement of the optimal current profile problem is

$$\max_{I(t)} \ \psi\left(I(t), [\mathrm{Fe}^{2+}]\right)$$

subject to

Continuous bioreactor model

$$1 \le I \le I_{sc}$$

$$1 \le I \le I_{\max}$$

$$\frac{dI}{dt} \geqslant 0$$

$$0 \le [\mathrm{Fe}^{2+}] \le [\mathrm{Fe}^{2+}]_{\max}$$

where I(t) is the current profile.

The objective function of the program was to maximize the function of current load and ferrous iron concentration profiles, while keeping the current and the concentration less than I_{sc} (or I_{max}) and $[Fe^{2+}]_{max}$, respectively.

Four different maximum ferrous iron concentrations (0.6, 0.8, 1.0, and 1.2 g/L) were chosen for finding the optimal current. The current profiles that maximize the objective function profiles are given in Figure 5. A rapid current increase at early times is observed in all profiles. This results in fast accumulation of ferrous iron in the system, the concentration of which reaches the acceptable maximum within the first 20–60 min. Once the current reaches its maximum value, I_{sc} or I_{max}, the ferrous iron generation rate becomes constant and its consumption rate in Eq. 13 gradually surpasses the generation rate, leading to a sharp decrease in ferrous iron concentration. Although the transient phase of operation is ended at almost the same time and with the same ferrous iron concentration for all runs, the lower maximum concentration provided better conditions (low ferrous iron concentration with less fluctuation) for the fuel cell to operate smoothly.

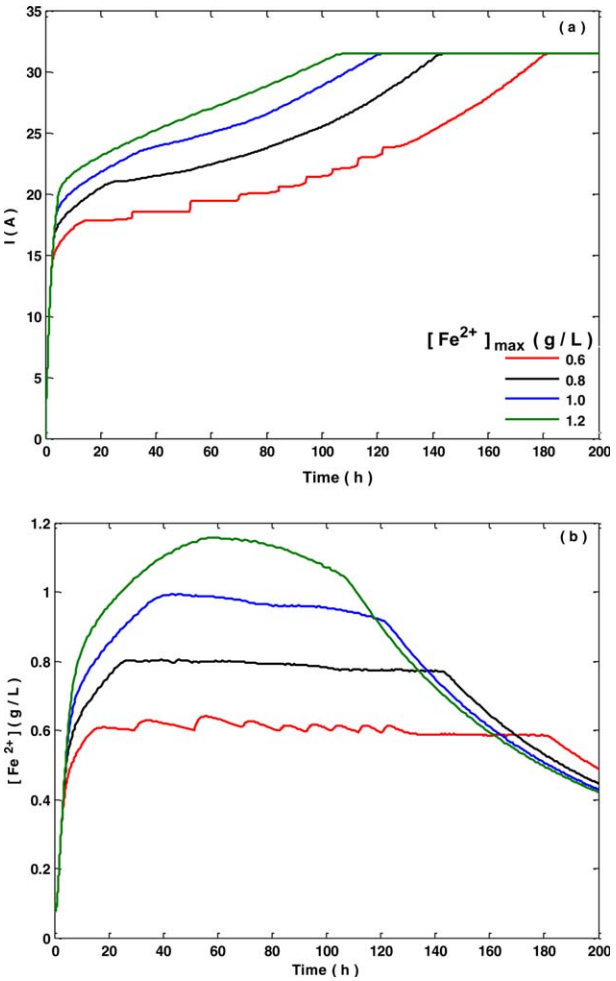

Figure 5. Simulation results for maximizing the value of ψ for various upper limits given for total ferrous iron concentration: (a) current profile; (b) total ferrous iron concentration profile.

[Color figure can be viewed in the online issue, which is available at wileyonlinelibrary.com.]

The validity of the model as well as the program developed can be assured, if the optimization program is combined with a mini-pilot-plant experiment in which the bacterial cells concentration, the ferrous iron concentration, and the pH are measured based on implemented optimal current profile. The mini-pilot-scale system used for open-loop control of a current load (based on the predicted optimal profile) was basically the same as that shown in Figure 1 except for the volume of the bioreactor and electrodes working area of the fuel cell, which were increased to 55 L and 400 cm^2,

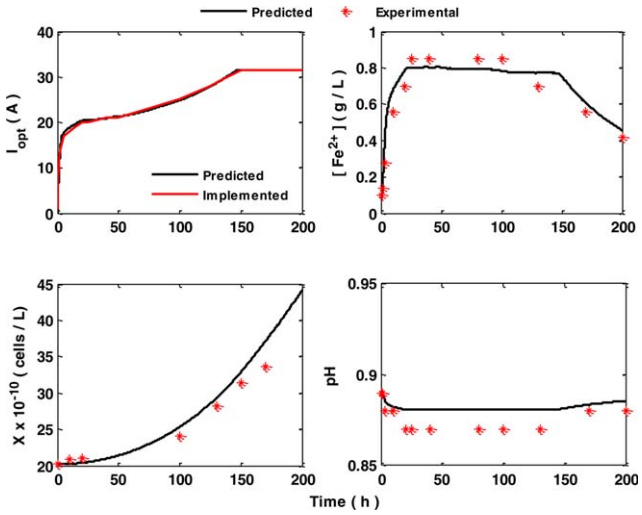

Figure 6. Comparison of experimental and simulation results for implemented current profile calculated for $[Fe^{2+}]_{max}$ = 0.8 g/L.

[Color figure can be viewed in the online issue, which is available at wileyonlinelibrary.com.]

respectively. The modified setup allowed to increase maximum attainable current to 35 A. However, the highest current could only be drawn, when the catholyte with highest redox potential was used. The initial conditions of the experiment are given in Table 2.

The result of the optimization calculations were tested in the mini-pilot-scale system, operated at current loads in accordance with the predicted profile for $[Fe^{2+}]_{max}$ = 0.8 g/L. The experimental results, compared with the simulations, are shown in Figure 6. As expected, the ferrous iron concentration rose rapidly to ~0.8 g/L, remained at that level for ~100 h, and then dropped sharply to its final level. Unfortunately, these changes affected performance of the fuel cell quite significantly and, at the ferrous iron peak concentration, a redox potential of the catholyte was not high enough to maintain the fuel cell voltage constant. It can be seen that here the pH is also overestimated; however, the differences between the predicted and measured values remain within the range of the pH measurement accuracy. In general, a good agreement between the experimental and predicted variables is an indication of an accurate estimation of a current profile.

The question may arise about how the ferrous iron concentration would change if the current was set at I_{sc} (or I_{max}) at the onset of experiment. The simulation results for these conditions indicate that at first the ferrous iron concentration would sharply increase up to almost 3 g/L within first 30 h of operation and then slowly decrease and reach 0.5 g/L after 200 h. This relatively low maximum concentration is accounted for by the high concentration of microorganisms, but it still, based on our previous experience, cannot provide favorable conditions for the maximum fuel cell performance. The simulations performed for the same initial values also showed that the conditions would deteriorate significantly if the bacterial cells concentration was decreased by only 10 or 15%, which would cause the maximum ferrous iron concentration to reach almost 5 and 32 g/L, respectively, with the pH plummeting down to 0.79 and 0.42, respectively. Such drastic condition changes in the bioreactor would lead to an unstable operation of the system. It should be mentioned that unstable operation refers to the conditions under which the pH drops below 0.6, inhibiting ferrous iron oxidation by microorganisms. Once the bacterial growth rate and ferrous iron oxidation decrease sharply, the ferrous iron concentration increases drastically, which leads to even larger drop in pH as well as tremendous reduction in a redox potential of the bioreactor liquid. The operation of the system would continue until no activity is observed from microorganisms and the fuel cell performance becomes nil.

Conclusions

A novel hybrid Fe^{3+}/Fe^{2+} redox flow fuel cell system using *L. ferriphilum* bacterium for catholyte regeneration was experimentally studied, and the model describing the system operation was developed and successfully tested. To take into account both the lag and growth phases of bacterial growth dynamics in the kinetic study, when estimating the kinetic parameters of a bioreaction involved, an exponential term of the growth profile was embedded in the model. Once the model was identified and validated through an autonomous run, a dynamic mathematical model representing the redox flow fuel cell system was developed to predict the ferrous iron concentration, bacterial cells concentration, and pH for any current drawn from the fuel cell. Three independent runs were performed theoretically and experimentally. Because the contribution of a lag phase in the developed model is well-established, the prediction ability of the model for pHs below lower limit (down to 0.6) was assured. Unfortunately, for all the studied cases, a slight overestimation of pH was observed. The issue likely is related to shortcomings of the model selected for estimation of activity coefficients of protons in the solution. However, notwithstanding the discussed limitations, the model was shown to adequately describe the parameters of the system, and showed a good agreement between the simulated and experimentally obtained values.

The results obtained also showed that the transient state of fuel cell operation requires an appropriate balance between the set current, ferrous iron concentration, and pH in the bioreactor to achieve stable-steady-state operation. The optimal current load profile was implemented through an open-loop control strategy and then validated by the results obtained experimentally from the redox flow fuel cell mini-pilot-scale system. Nonetheless, further studies on applicability of the developed model to scaling up the process as well as use of other models to estimate the activity coefficients of ions are highly recommended.

Notation

a = ionic activity
c, d, f = model constants
E_h = redox potential of solution, mV
E' = formal redox potential, mV
F = Faraday constant, C/mol
$[Fe]_t$, $[Fe^{2+}]$, $[Fe^{3+}]$ = total, ferrous, and ferric iron concentrations, g/L
G_r^o = standard Gibbs free energy for chemical reactions
I = electrical current, A
I_m = ionic strength of the solution (on molality basis)
k = exponential constant for the lag phase, 1/h
K = equilibrium constant
K_1, K_2 = kinetic constants

K_s = half-saturation constant, g/L
m = molality, mol/kg_{water}
M = molecular mass, g/mol
n = numbers of electrons exchanged in electrochemical reaction
q_s, q_{max} = specific and maximum specific ferrous iron bio-oxidation rate, g/(L h)
R = the universal gas constant, J/(mol K)
t = time, h
T = absolute temperature, K
v = circulation rate of solution through the fuel cell, L/h
V = volume, L
X = microbial cell concentration, cells/L
Y = biomass yield coefficient, cells/g_{Fe}
z = charge of ions

Greek letters

α, β = constants
γ = activity coefficient of ions
Φ, ψ = objective functions for optimization programs
μ = specific growth rate, 1/h
ρ, = density of solution, kg/$L_{solution}$
υ = stoichiometric coefficients in chemical reactions
ω = weight factor for optimization programs

Subscripts and superscripts

b = bounded state of ion in the solution
f = free state of ion in the solution
L = lower limit
max = maximum
s = selected
sc = short circuit
t = total
U = upper limit
o = initial value of variable

Literature Cited

1. Karamanev DG, Glibin VP, Dobreff PV. Fuel cell bioreactor. US Patent 10.1002/20090305083, 2009.
2. Karamanev DG, Pupkevich VR, Hojjati H. Bio-fuel cell system. US patent 10.1002/20100040909, 2010.
3. Das SK, Bansode AS. Heat and mass transfer in proton exchange membrane fuel cells-A review. *Heat Transfer Eng*. 2009;30:691–719.
4. Siegel C. Review of computational heat and mass transfer modeling in polymer-electrolyte-membrane (PEM) fuel cells. *Energy*. 2008;33:1331–1352.
5. Tao WQ, Min CH, Liu XL, He YL, Yin BH, Jiang W. Parameter sensitivity examination and discussion of PEM fuel cell simulation model validation, Part I. Current status of modeling research and model development. *J Power Sources*. 2006;160:359–373.
6. Bond PL, Druschel GK, Banfield JF. Comparison of acid mine drainage microbial communities in physically and geochemically distinct ecosystems. *Appl Environ Microbiol*. 2000;66:4962–4971.
7. Boon M, Brasser HJ, Hansford GS, Heijnen JJ. Comparison of the oxidation kinetics of different pyrites in the presence of *Thiobacillus ferrooxidans* or *Leptospirillum ferrooxidans*. *Hydrometallurgy*. 1999;53:57–72.
8. Rawlings DE, Tributsch H, Hansford GS. Reasons why "*Leptospirillum*"-like species rather than *Thiobacillus ferrooxidans* are the dominant iron-oxidizing bacteria in many commercial processes for the biooxidation of pyrite and related ores. *Microbiology*. 1999;145:5–13.
9. Meruane G, Salhe C, Wiertz J, Vargas T. Novel electrochemical-enzymatic model which quantifies the effect of the solution on the kinetics of ferrous iron oxidation with *Acidithiobacillus ferrooxidans*. *Biotechnol Bioeng*. 2002;80:280–288.
10. Ojumu TV, Hansford GS, Petersen J. The kinetic of ferrous-iron oxidation by *Leptospirillum ferriphilum* in continuous culture: the effect of temperature. *Biochem Eng J*. 2009;46:161–168.
11. Gao J, Zhang C, Wu X, Wang H, Qiu G. Isolation and identification of a strain of *Leptospirillum ferriphilum* from an extreme acid mine drainage site. *Ann Microbiol*. 2007;57:171–176.
12. Ozkaya B, Nurmi P, Sahinkaya E, Kaksonen AH, Puhakka JA. Temperature effects on the iron oxidation kinetics of a *Leptospirillum ferriphilum* dominated culture at pH below one. *Adv Mat Res*. 2007;20–21:465–468.
13. Penev K, Karamanev DG. Batch kinetics of ferrous iron oxidation by *Leptospirillum ferriphilum* at moderate to high total iron concentration. *Biochem Eng J*. 2010:50:54–62.
14. Moraw F, Fatih K, Wilkinson D, Girard F. Evaluation of the Fe(III)/Fe(II) redox fuel cell cathode couple in a bioelectrolytic solution. *Adv Mat Res*. 2006;15–17:315–320.
15. Ojumu TV, Petersen J, Searby GE, Hansford GS. A review of rate equations proposed for microbial ferrous-iron oxidation with a view to application to heap bioleaching. *Hydrometallurgy*. 2006;83:21–28.
16. Bryan CG, Davis-Belmar CS, van Wyk N, Fraser MK, Dew D, Rautenbach GF, Harrison STL. The effect of CO_2 availability on the growth, iron oxidation and CO_2-fixation rates of pure cultures of *Leptospirillum ferriphilum* and *Acidithiobacillus ferrooxidans*. *Biotechnol Bioeng*. 2012;109:1693–1703.
17. Pupkevich V, Glibin V, Karamanev D. The effect of ferric ions on the conductivity of various types of polymer cation exchange membrane. *J Solid State Electrochem*. 2007;11:1429–1434.
18. Ghauri MA, Okibe N, Johnson DB. Attachment of acidophilic bacteria to solid surfaces: the significance of species and strains variations. *Hydrometallurgy*. 2007;85:72–80.

Manuscript received Jan. 30, 2012; and revision received Oct. 23, 2012.